Kidney International, Vol. 42 (1992), pp. 136–147

Glomerular damage after uninephrectomy in young rats. I. Hypertrophy and distortion of capillary architecture

MICHIO NAGATA,[1] KARL SCHÄRER, and WILHELM KRIZ

Institut für Anatomie und Zellbiologie und Kinderklinik der Universität Heidelberg, Heidelberg, Germany

Glomerular damage after uninephrectomy in young rats. I. Hypertrophy and distortion of capillary architecture. Uninephrectomy (UNX) results in a higher incidence of focal glomerular sclerosis (FGS) in young rats than it does in adults. The reason for this higher susceptibility in young animals is not fully understood, but this does suggest that UNX in young rats may represent a particularly promising model in which to study the development of FGS. In the present study 10-day-old rats were subjected to UNX. After 4, 12 and 24 weeks, glomerular hypertrophy, structural lesions and function were analyzed in comparison with sham-operated controls. Up to the twelfth week, remnant kidney growth and glomerular growth proceeded in parallel; thereafter, kidney growth ceased, whereas glomerular growth continued undiminished. Twenty-four weeks after UNX, glomerular tuft volume in experimental animals exceeded that in controls by 80%. Twelve weeks after surgery, total GFR in UNX rats was approximately 80% of that in controls, a value maintained until the end of the observation period. Twenty-four weeks after surgery, heavy proteinuria was present in UNX animals. Structural abnormalities in glomeruli of UNX animals were already encountered 12 weeks after surgery; they were present to a much lesser extent in controls. In UNX animals these proceeded to the FGS stage by the end of the observation period. Three major groups of glomerular lesions were observed: (1) changes in the width and shape of glomerular capillaries. (2) changes in podocyte structure, and (3) tuft adhesions to Bowman's capsule with or without segmental sclerosis. The structural changes are analyzed in this and an accompanying paper [1]. The present paper deals with the widespread formation of irregular, giant capillary loops. They occur predominantly at the tuft periphery with a clear predilection for the vascular pole region. They are not a result of compensatory growth, but rather an expansion of single capillaries due to failure of the mesangium. Local disconnection of the mesangium from its anchoring points at the GBM leads to bulging and "coalescence" of capillary loops, resulting in abnormally-shaped vascular channels. This process is associated with a rearrangement of the corresponding mesangium. In our view, the appearance of dilated capillaries represents a local event pivotal to the development of more severe lesions, such as tuft adhesions and FGS.

In recent years glomerular hypertrophy has come to be widely considered as a crucial forerunner of glomerulosclerosis [2, 3]. In young rats, uninephrectomy (UNX) results in a more pronounced compensatory hypertrophy of the remnant kidney than in adults [4] followed by a higher incidence of focal and segmental glomerulosclerosis (FGS) [5–8]. The reason for this greater susceptibility of young animals to UNX is not fully understood. We used young rats because we thought that due to their higher susceptibility they represent a particularly promising model in which to study the development of FGS.

The focal and segmental distribution of the lesions in glomerular sclerosis suggests the existence of a decisive local contribution to the evolution of glomerular injury. The present study provides a detailed structural analysis of the process of glomerular hypertrophy and the subsequent development of tuft lesions.

This study suggests that glomerular hypertrophy contributes to local mesangial failure resulting in capillary dilatation. In conjunction with maladaptive changes in podocyte structure (described in the accompanying paper [1]) the distortions we describe in tuft structure take on pathogenetic relevance in the evolution of tuft adhesions and segmental sclerosis.

Methods

Forty-four male Sprague-Dawley (SD) rats were uninephrectomized (left kidney) or sham-operated at ten days of age, a time when nephrogenesis has just been completed [9]. After the operation, they were returned to their mothers until weaning at 21 days. The mothers and their offspring were fed standard rat chow and water *ad libitum*. Four (UNX 6; sham 6), twelve (UNX 8; sham 6) and twenty-four weeks (UNX 8; sham 6) after uninephrectomy or sham operation, rats were studied to estimate renal functional and structural parameters. In addition, eight rats (4 UNX, 4 controls) were used to prepare glomerular vascular casts at 16 weeks after operation.

Glomerular filtration rate (GFR) and effective renal plasma flow (ERPF)

GFR and ERPF were assessed by a previously reported method using a single injection of ^{99m}Tc-DTPA and ^{125}I-hippurate [10]. Briefly, after determining their body weight, rats were superficially anesthetized with ether for about 15 seconds to allow intravenous injection of the radioactive indicators via the sublingual vein. The amount of radioisotope injected was estimated by the difference in weight of the syringe before and after injection. After one hour the rats were anesthetized again for

[1] Present address: Department of Pediatric Nephrology, Kidney Center, Tokyo Women's Medical College, 8-1 Kawada-cho, Shinjuku-ku, Tokyo, Japan.

Received for publication September 16, 1991
and in revised form February 21, 1992
Accepted for publication February 24, 1992

blood sampling from the orbital plexus. Two hundred microliters of plasma of each animal were measured by gamma-scintillation counting. GFR and RPF were calculated with the following formula:

$$C = (V/t) \times \log_n(P_0/P_t)$$

where C is the clearance ERPF (ml/min) of ^{99m}Tc-DTPA for GFR or ^{125}I-hippurate for V is the volume of distribution of either substance (ml), calculated from body weight as described by Provoost and co-workers [10]. For calculation of ERPF in rats of more than 400 g body weight, volume of distribution of ^{125}I-hippurate was estimated as the volume of distribution for ^{99m}Tc-DTPA + 5 ml (Provoost, unpublished observation 1991). P_0, the concentration of radioactivity at the time of injection (cpm/ml), was calculated from the volume of distribution V(ml) and I, the amount of radioactivity (cpm) injected. P_t is the concentration of radioactivity in the plasma sample (cpm/ml) taken t = 60 minutes after injection. The values were expressed as absolute GFR (ml/min), GFR per kidney weight (ml/min/g), and GFR per total glomerular tuft volume (ml/min/mm^3). The latter value was calculated by using the mean tuft volume of each animal (see below) and an anticipated equal number of 30,000 glomeruli per kidney [11] (thus a total of 30,000 in UNX animals, 60,000 in controls). According to previous reports nephrogenesis in rats is complete within 10 days after birth [9] and does not resume after UNX even in young animals [4, 12]. For urinary protein excretion measurements, animals were kept in metabolic cages for 24 hours and the urine was collected. During this time, animals were not fed. Protein concentration was measured by the Coomassie blue protein-dye binding method [13].

Tissue fixation and processing

On the last day of the experiment the body weight of each animal was determined. Afterwards the kidneys were fixed by total body perfusion. Under pentobarbital anesthesia (7.2 mg/100 g body wt), a cannula was inserted retrograde into the abdominal aorta. Without prior flushing of the blood, the animals were directly perfused with a 1.5% glutaraldehyde, phosphate buffer solution (pH 7.4) supplemented with 0.05% picric acid. Perfusion was performed at a pressure of 200 mm Hg for three minutes as described previously [14]. Afterwards the kidneys were removed and weighed. The right kidney was cut into several pieces and postfixed for 48 hours in the same fixative used for perfusion.

For electron microscopy and morphometry in semithin sections, approximately 2 mm^3 cubes of cortical tissue (containing the cortex from the surface to outer stripe) were cut out from a midpiece of the kidney, postfixed in 1% osmium tetroxide for one hour, dehydrated in a graded series of ethanols and embedded in epoxy resin by standard procedures. Additional tissue blocks were treated by a modified postfixation and staining technique which minimizes treatment with osmium tetroxide and uses tannic acid as a contrast agent [15]. Semithin and ultrathin sections were cut on a Ultracut E microtome (Cambridge Instruments, Nußloch, Germany). Semithin sections were stained with methylene blue and examined by light microscopy. Ultrathin sections were stained with uranyl acetate and lead citrate and observed in a Philips 301 electron microscope at 80 KV. A second midpiece of the kidney was embedded in paraffin (Paraplast®) by standard procedures. Coronal sections of 3 μm thickness were cut, stained by the periodic acid-Schiff technique and examined by light microscopy.

Qualitative evaluation of structural changes

Frequency of focal and segmental glomerular sclerosis (% GS) was determined in paraffin sections in superficial glomeruli according to previously reported procedures [16]. In each animal, all such glomerular profiles contained in three or four coronal sections were considered (approximately 420 glomeruli per animal). Profiles were considered sclerotic when the tuft contained an area with collapsed capillary loops together with an accumulation of hyalin material.

By inspection of 1 μm sections in the light microscope, two capillary patterns could be distinguished: a uniform pattern, in which most of the capillary profiles were roughly of the same apparent diameter, and a heterogeneous pattern, in which capillary profiles were seen which were clearly larger than the majority of capillaries and, in addition, which frequently appeared to be of abnormal shape. The frequency of heterogeneous glomerular profiles was estimated in experimental and control animals by analyzing approximately 60 superficial glomerular profiles in each animal. Glomerular profiles were considered heterogeneous when at least three abnormally large capillary profiles were encountered. Capillary profiles were considered "clearly larger" if the diameter was at least twice as large as in normal profiles; they were considered "abnormally shaped" if such profiles could not have resulted from sectioning a normal capillary loop.

The location of dilated capillaries within the tuft was determined in 1 μm sections of all experimental animals of the 12-week UNX group. All meridional sections through glomeruli (including the vascular pole) were photographed. In the photographs all dilated capillaries were marked and evaluated for location with respect to the vascular pole. In this regard, a capillary was considered related to the vascular pole if any part lay within a circle having the vascular pole as a center and a radius of about one third of the maximal tuft diameter.

Morphometric procedures

Mean glomerular tuft volume ($\overline{V}_G$) of each animal was calculated according to a frequently used procedure [17–19] described by Weibel [20]. In epon-embedded 1 μm thick sections the glomerular tuft area (A_G) was measured in randomly sampled glomerular profiles of superficial glomeruli using a semi-automatic image analysis system (VIDS IV, Ai Tektron, Düsseldorf, Germany) as described previously [19]. On average 65 profiles were analyzed in each animal. Since glomerular size decreases with the progression of glomerulosclerosis [3, 21], glomerular profiles with recognizable sclerotic lesions were excluded from the measurements.

The $\overline{V}_G$ was calculated according to the formula [20].

$$\overline{V}_G = (\beta/k)(\overline{A}_G)^{3/2}$$

where β = 1.38 is the shape coefficient and k = 1.1 is the size distribution coefficient for spheres.

Capillary length density [L_V(CAP)] and absolute length of capillaries per glomerulus of average volume (L_{CAP}) were estimated by the previously described formulas [20]:

$$L_V(CAP) = 2 \times N_{CAP} \div (A_T) \text{ and}$$

$$\bar{L}_{CAP} = \bar{L}_V(CAP) \times \bar{V}_G$$

N_{CAP}, the number of capillary profiles, and A_T, the corresponding tuft area, were determined in light micrographs (final magnification 1550) of 10 glomerular profiles per animal, randomly sampled in epon-embedded 1 μm thick sections. (The same photos were later used for the determination of N_V(PO) in the accompanying paper [1].) The mean of each animal (L_VCAP) was determined and—together with the mean glomerular tuft volume (V_G; as determined above)—used for the calculation of L_{CAP}.

Scanning electron microscope (SEM) study of glomerular casts

Eight additional male SD rats (4 control, 4 UNX) were used for the study of glomerular vascular casts by scanning electron microscopy (SEM). Sixteen weeks after UNX or sham operation, the animals were anesthetized and a cannula was inserted in the abdominal aorta as described above. Immediately after flushing of the blood with PBS (1 min perfusion at a pressure of 200 mm Hg), 2.5 ml of methacrylate injection medium (Mercox, CL-2B, Japan Vilene Hospital, Tokyo, Japan) were rapidly injected by hand. Just before injection, a curing agent (MA, Japan Vilene Hospital) was added to the injection solution. After the injection, the renal artery and vein were clamped and the kidneys were removed and allowed to polymerize for 30 minutes at room temperature. The kidneys were then allowed to polymerize for additional two hours in 40°C water, followed by digestion with 15% KOH to remove all tissue. The resulting vascular casts were rinsed with water and dried at room temperature. Specimens were mounted on aluminum stubs with silver conductive paint, sputter-coated with gold (100 Å), and examined in a Philipscan 500 scanning electron microscope operating at 25 kV.

Statistics

Values for glomerular tuft volume and for capillary parameters were calculated as means ± SD for individual groups. Statistical significance of differences among groups was tested with Student's *t*-test. $P < 0.05$ was considered significant for all statistical comparisons. Linear regression analysis was employed to examine to correlation between mean glomerular tuft volume and frequency of FGS in animals 24 weeks after UNX.

Results

Functional measurements

During the entire observation period, total glomerular filtration rate (GFR) in UNX animals was significantly lower than total GFR in sham-operated animals. GFR per kidney, on the other hand, was significantly higher (Table 1 and 2). No differences in GFR per kidney weight were found between the groups at any age. In both groups GFR/KW increased by a factor of approximately 2.5 between 4 and 12 weeks; by 24 weeks the value in both groups had decreased slightly. GFR per total glomerular tuft volume at 4 and 12 weeks tended to be higher in UNX animals than in sham-operated animals; at 24 weeks, this value tended to decline in UNX animals relative to controls (Table 2).

Table 1. Morphometric parameters of superficial glomeruli

	$\bar{V}_G$ $\mu m^3\ 10^6$	$\bar{L}_{CAP}$ mm	$\bar{L}_V$(CAP) m/mm^3
4 weeks			
UNX ($N = 6$)	0.67 ± 0.09[a]	7.2 ± 0.9[b]	10.6 ± 0.9
Sham ($N = 6$)	0.51 ± 0.07	6.0 ± 0.7	11.6 ± 0.6
12 weeks			
UNX ($N = 8$)	2.28 ± 0.3[a,c]	18.0 ± 2.6[a,c]	7.8 ± 0.7[b,c]
Sham ($N = 6$)	1.43 ± 0.2[c]	12.2 ± 1.2[c]	8.8 ± 0.5[c]
24 weeks			
UNX ($N = 8$)	3.67 ± 0.6[a,d]	24.2 ± 2.8[a,d]	6.7 ± 0.9[b,e]
Sham ($N = 6$)	2.07 ± 0.4[d]	16.3 ± 3.1[d]	7.8 ± 0.6[e]

All values are expressed as average ± SD. Abbreviations are: $\bar{V}_G$, average glomerular tuft volume; $\bar{L}_V$(CAP), average glomerular capillary length density; $\bar{L}_{CAP}$, absolute length of glomerular capillaries per glomerulus. [a,b], UNX vs. sham operation; [c, d and e], comparisons between different manifestation times within the sham operation or UNX group.

[a] $P < 0.01$; [b] $P < 0.05$; [c] $P < 0.01$, 4 vs. 12 weeks

[d] $P < 0.01$, 12 vs. 24 weeks; [e] $P < 0.05$, 12 vs. 24 weeks

Similar changes were found in effective renal plasma flow (ERPF): Total ERPF was lower and ERPF per kidney was higher in UNX animals than in sham-operated controls. ERPF per kidney weight in UNX also tended to be higher (Table 2).

Urinary protein excretion was in the normal range in both animal groups at four weeks after the operation. After 12 and 16 weeks, a moderate but clearly elevated protein excretion was noted in UNX animals. A heavy proteinuria was observed after 24 weeks in UNX animals, while controls continued to show a protein excretion within the normal range (Table 2).

Body, kidney and glomerular growth

Up to 12 weeks after operation, differences in body weight between sham-operated and experimental animals were not observed; thereafter body growth in the experimental group decelerated, resulting in significant growth retardation after 24 weeks (Fig. 1). Single kidney weight was significantly increased in UNX animals by four weeks after operation compared with sham-operated animals. This difference increased until 12 weeks after the operation; afterwards, no further kidney growth was observed in UNX animals (Fig. 1). Kidney growth in sham-operated animals was constant over the entire observation period, but the individual kidneys never reached the size of the single kidneys in UNX animals.

Glomerular tuft growth was increased in experimental animals compared to controls as early as four weeks after UNX. Despite the cessation of kidney growth in UNX animals, growth of glomeruli proceeded unabated until the end of this experiment (Fig. 1b). Glomerular tuft volume in UNX animals at 24 weeks was 177% of that in controls, kidney weight 136% of the control value (Fig. 1, Table 1).

Glomerular tuft growth was accompanied by lengthening of glomerular capillaries (Table 1), but growth of the glomerular tuft as a whole and of the capillaries did not fully parallel each other. Four weeks after surgery, capillary density [$\bar{L}_V$(CAP)] was not different between UNX animals and sham-operated controls; thereafter capillary density decreased in both groups.

Table 2. Kidney function and protein excretion

	GFR *ml/min*	GFR/kidney wt *ml/min/g*	GFR/V_G *ml 10^{-2}/min/mm³*	ERPF *ml/min*	ERPF/kidney wt *ml/min/g*	Protein excretion *mg/day*
4 weeks						
UNX	0.53 ± 0.1	0.39 ± 0.1	2.61 ± 0.52	1.7 ± 0.4	1.3 ± 0.4	1.4 ± 0.2
Sham	0.76 ± 0.2[a]	0.38 ± 0.1	2.15 ± 0.39	2.1 ± 0.3	1.0 ± 0.1	2.0 ± 0.4
12 weeks						
UNX	2.7 ± 0.2	0.92 ± 0.1	3.74 ± 0.58	4.9 ± 0.2	1.7 ± 0.2	20 ± 4[a]
Sham	3.4 ± 0.1[b]	0.93 ± 0.1	3.31 ± 0.35	5.9 ± 0.2[b]	1.6 ± 0.3	8.3 ± 6
16 weeks						
UNX	2.6 ± 0.2	NE	NE	4.7 ± 0.4	NE	30 ± 7[b]
Sham	3.2 ± 0.2[b]	NE	NE	5.1 ± 0.3[a]	NE	6.8 ± 3
24 weeks						
UNX	2.6 ± 0.2	0.85 ± 0.1	2.29 ± 0.51	5.2 ± 0.2	1.7 ± 0.2[a]	93 ± 21[b]
Sham	3.5 ± 0.2[b]	0.81 ± 0.1	2.58 ± 0.65	6.6 ± 0.4[b]	1.5 ± 0.2	10 ± 4

Values are expressed as average ± SD. Abbreviations are: GFR, glomerular filtration rate; ERPF, effective renal plasma flow; kidney wt, kidney weight; V_G, glomerular tuft volume; NE, not examined.
[a] $P < 0.05$, [b] $P < 0.01$, comparisons between UNX and sham-operated rats within the same time group.

The decrease in capillary density was more pronounced in the hypertrophied glomeruli of UNX animals than in sham-operated animals.

Mean glomerular volume per body weight did not change significantly with growth in control animals (Fig. 1c). In UNX animals this value increased from slightly above that of controls after four weeks to approximately twice the control value by the end of the observation period.

Structural changes

Along with the hypertrophic growth of glomeruli in UNX animals, several kinds of structural changes were observed increasing in frequency and severity with time. Four weeks after UNX, changes were only rarely seen, after 12 weeks changes were already widespread, including severe lesions such as tuft adhesions to Bowman's capsule. Twenty-four weeks after UNX more than 75% of all glomerular profiles exhibited abnormalities in tuft structure, which had focally proceeded to segmental sclerosis. The frequency of sclerosis among the animals in this group ranged between 0 and 14.3%, mean 5.3% (evaluated in superficial glomeruli). A close correlation in the mean glomerular tuft volume and frequency of FGS in rats 24 weeks after UNX ($N = 8$, $r = 0.684$) was found.

The structural changes can be subsumed under three groups: (1) changes in the width and shape of glomerular capillaries associated with changes in the distribution of the associated mesangium; (2) various changes in podocyte structure; and (3) tuft adhesions to Bowman's capsule with or without segmental sclerosis. Surprisingly, mesangial expansion was not encountered as a common lesion; it was only found in conjunction with established tuft adhesions. The present paper describes and analyzes the first group of lesions; the latter two groups will be presented in the accompanying paper [1].

Changes in shape and width of glomerular capillaries

Changes in shape and width of glomerular capillaries can most clearly be seen by SEM of vascular casts (Fig. 2). Glomerular casts of sham-operated animals exhibited the well-known anastomosing network of capillaries; generally the capillaries were fairly uniform in diameter (Fig. 2a). Glomerular casts of UNX animals clearly showed the hypertrophy of the tufts. These exhibited two capillary patterns. In the majority of tufts, the capillary loops were fairly uniform in diameter, resembling in size and shape those of normal glomeruli (Fig. 2b). Frequently, however, glomerular tufts were encountered which contained abnormally shaped loops with remarkably large calibers (Fig. 2c and d). These dilated capillaries were frequently found in clusters in one part of the tuft, more often near the vascular pole than at any other location, involving the first branches of the afferent arteriole. Some glomerular profiles with such a heterogeneous capillary pattern were also found in controls.

By LM and TEM these dilated capillaries were equally easy to see as large and abnormally-shaped capillary profiles (Figs. 3 and 4). They were frequently associated with local changes in the arrangement of the mesangium and with podocyte lesions. The structural variety of such dilated capillary profiles was great; differences in form due to the plane of section added considerably to the actual diversity.

To understand the formation of such abnormally-shaped vascular channels one has to consider the specific support of glomerular capillaries. Their shape and course is stabilized exclusively by the centripetal fixation of the GBM to the mesangium. If those connections are disrupted, the mesangium retracts followed by the dilation and "coalescence" of capillary loops; capillary channels of abnormal shape and width result. We interpret capillary arrangements, as seen in Figure 5, as immediate precursors of a further step in the "coalescence" of two capillaries into a single giant capillary. The thin mesangial bridge (covered on both sides by an endothelial layer) between the two capillary profiles represents the outermost part of a mesangium which is in the process of retracting. The mesangium loses its fixation points at one or at both sides of the bridge and moves towards the center of the lobule axis. The result is a deformed capillary loop with a wide lumen (Figs. 4 and 6).

The corresponding mesangium changed its overall shape and location as well. The mesangium retracted; if at least two capillary loops were involved, the corresponding mesangium retracted into a centripetally located agglomeration which often protruded into the newly established vascular channel (Fig. 4 and 6). In these rearranged mesangial aggregates (Fig. 6b), mesangial cell structure appeared quite simplified: most of

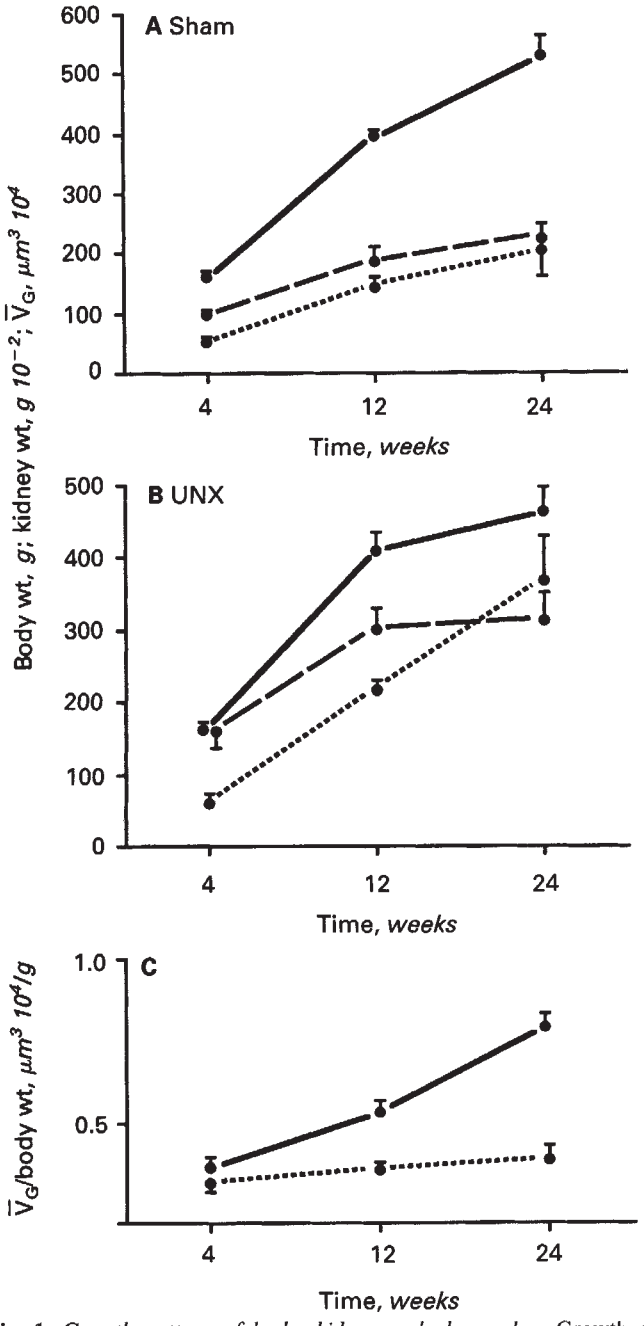

Fig. 1. *Growth pattern of body, kidney and glomerulus.* Growth of body and kidney were estimated by weight (body wt and kidney wt, respectively), glomerulus growth by mean glomerular tuft volume (V_G). Upper panel: In sham-operated rats, body growth (continuous line), kidney growth (hatched line) and glomerulus growth (dotted line) proceeded fairly in parallel. Middle panel: In UNX animals, a similar growth pattern as in controls was seen until 12 weeks after surgery; thereafter body growth decreased, kidney growth was arrested, whereas glomerulus growth continued undiminished. Lower panel: In controls (hatched line), the ratio between glomerular tuft volume and body weight remained constant during growth, in UNX rats (continuous line), it increased continuously. Number of animals: $N = 6$, except the 12 and 24 weeks UNX groups with $N = 8$. Values are depicted ± SD.

the cell processes appeared to have lost their usual connections to the GBM. Between the cells and cell processes a moderate amount of mesangial matrix, including clusters of microfibrils, were found. Toward the capillary lumen, the newly established mesangial areas were always completely covered by endothelium. Discontinuities in the endothelial layer were not observed (Fig. 6b), not even in the largest capillary channels.

The frequency of glomerular profiles with distorted and widened capillaries is shown in Figure 7. Profiles with such deformed capillaries were already found after four weeks, even in the sham-operated group. They became a more conspicuous attribute in the UNX group 12 weeks after nephrectomy. By 24 weeks they were seen in almost 50% of the glomerular profiles in the UNX group, an increase was also noted in the sham-operated animals but less so than in UNX animals.

These kinds of dilated and distorted capillaries were predominantly found in the periphery of the tuft with a conspicuous predilection of the capillary loops at the vascular pole. Out of the 298 dilated capillary loop profiles encountered in meridional sections through glomeruli (which include the vascular pole) 166 (that is, 56%) were located at the vascular pole, and probably comprised primary branches of the afferent arteriole.

Discussion

In young rats, UNX leads to a relatively high frequency of focal glomerular sclerosis [5, 8]. In humans as well, a single kidney at birth seems more predisposed to decreasing renal function and to sclerosis than a kidney remaining after unilateral nephrectomy during adulthood [22]. The reason for this higher susceptibility in kidneys of younger individuals is not known. Hypertrophy has come to be widely accepted as a crucial forerunner of sclerosis. Previous studies [3, 23] have demonstrated a close correlation of glomerular size to incidence of sclerosis in experimental models in adult rats. In young animals a more vigorous hypertrophic response to UNX has been suggested to account for the increase in susceptibility [8]. However, other factors may also come into play. As shown recently by Jelinek and co-workers [24], UNX in young rats compromises renal sodium excretion, predisposing them to volume expansion and, possibly, hypertension, which accelerates glomerular injury.

The present study does not examine the reasons for the higher susceptibility of young rats. We simply take advantage of it, using UNX in young rats as a favorable model in which to study the development of FGS. In contrast to models in adult rats, UNX alone is sufficient to produce FGS; additional experimental manipulation or treatment is unnecessary; moreover, immune mechanisms are not involved in the pathogenesis of FGS in this model.

Structure-function correlations

UNX in 10-day-old rats induced—as expected—a pronounced hypertrophic growth of the remnant kidney. Up to 12 weeks after UNX, kidney and glomerulus growth proceeded in parallel. GFR per kidney weight was exactly the same as in controls, suggesting that the underlying growth pattern is similar in normal and early hypertrophic growth. By 24 weeks after UNX, however, a number of differences between UNX animals and controls were evident. Most noticeable was the fact that kidney growth and glomerular growth had been dissociated: no further increase in kidney weight was observed from the 12th week, whereas glomerular growth continued undiminished (Fig. 1, Table 1). This observation is corroborated by experiments in

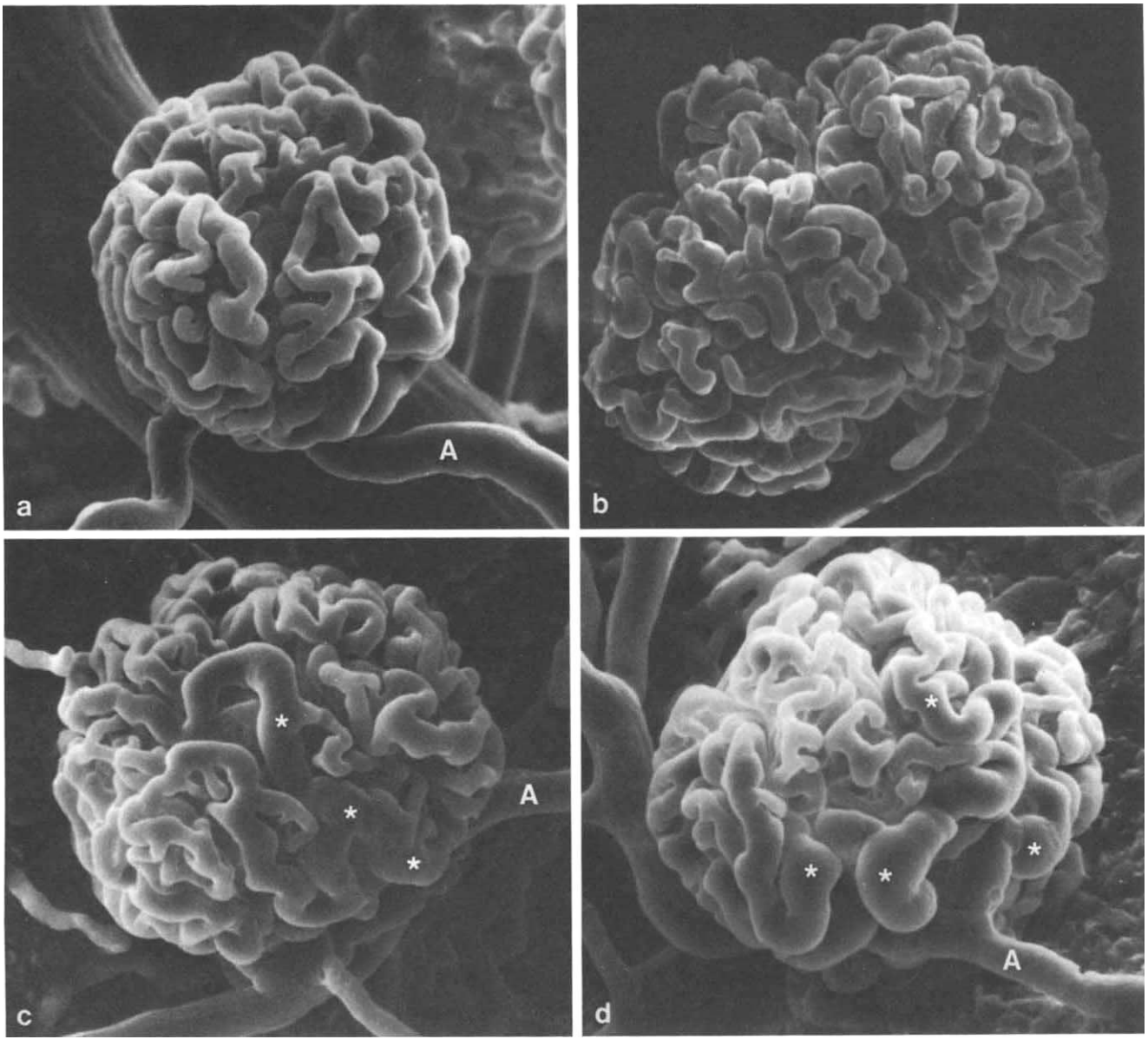

Fig. 2. *Scanning electron micrographs of glomerular vascular casts 16 weeks after surgery.* **(a)** A glomerulus from a sham-operated rat showing a fairly uniform capillary pattern. **(b–d)** Glomeruli from UNX rats are clearly larger than in (a). (b) Uniform capillary pattern: most of the capillaries are of approximately the same size. (c and d) Heterogenous capillary patterns with abnormally shaped and dilated capillary channels on the surface of the tuft (asterisks); in both profiles primary branches of the afferent arteriole (A) are involved. (a–d) ×~320.

SV 40 transgenic mice [25] as well as in transgenic mice carrying an additional gene for growth hormone [26], which have provided evidence that total kidney growth (reflecting primarily tubular growth) and glomerulus growth are regulated independently and appear to have different thresholds for activation following UNX.

Total GFR (GFR per animal) in UNX rats did not further increase during the period between 12 and 24 weeks; total GFR in controls increased only slightly. Thus, the UNX animals maintained a GFR of almost 80% of that in controls until the end of the observation period. This was apparently the result of a high ERPF (Table 2). Due to arrest of body and kidney growth in UNX animals at the 12th week, GFR per body weight (not shown) or per kidney weight in UNX animals even appeared to improve 24 weeks after UNX when compared with the respective values in controls (Table 2). This is in agreement with previous studies [5, 27] in which GFR in UNX animals remains fairly stable for up to six months after UNX.

The picture changes considerably when GFR is expressed per total glomerular volume (Table 2). From 12 to 24 weeks after surgery, this value decreased in both experimental and control

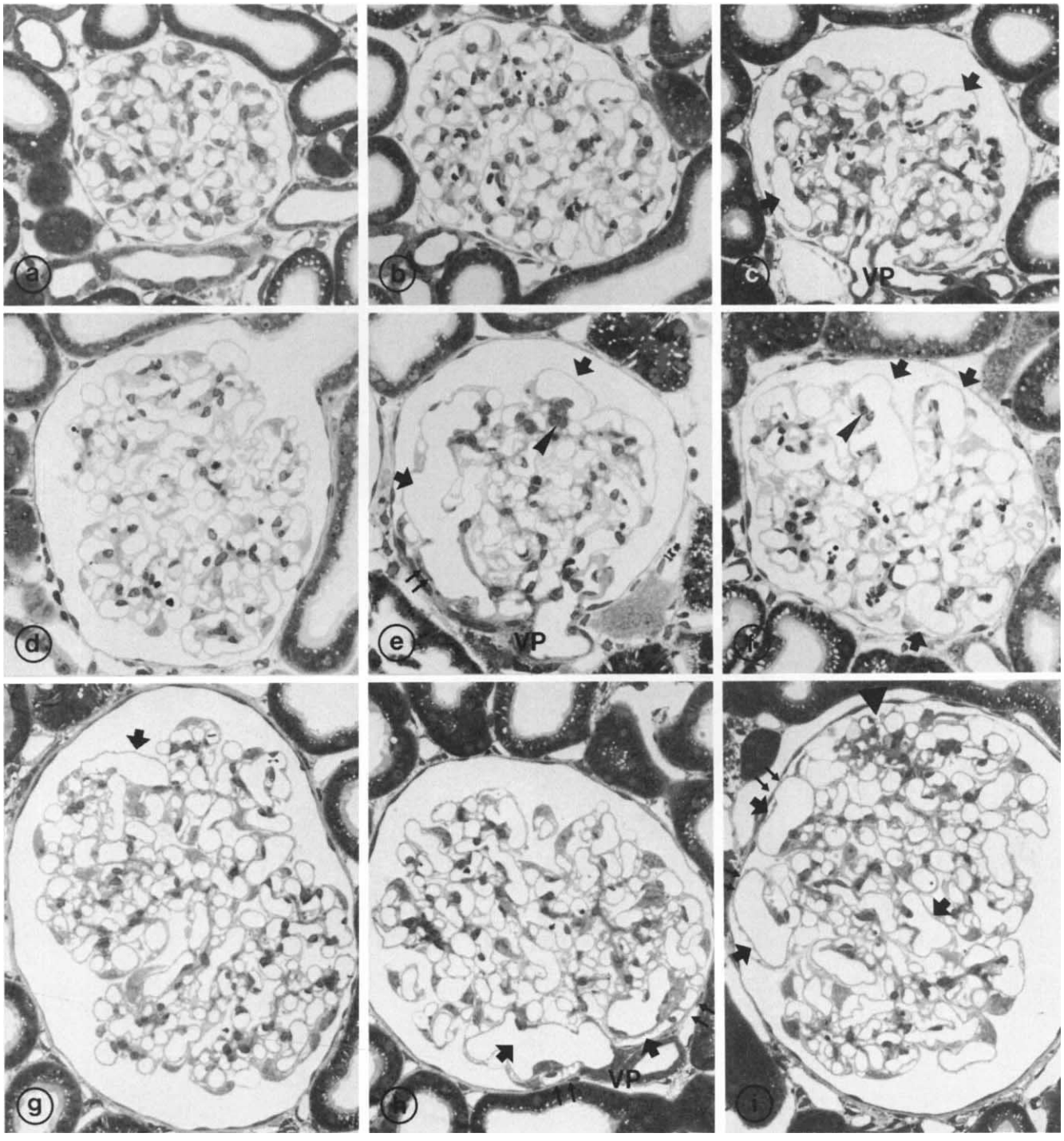

Fig. 3. *High resolution light microscopy of glomeruli.* **(a)** Rat, 4 weeks after sham-operation; all capillary profiles are of approximately the same size. **(b and c)** Rats, 4 weeks after UNX; glomeruli are somewhat larger than in controls, major differences in tuft structure are not seen, but individual capillaries (arrows in c) tend to increase in diameter. **(d–f)** Rats, 12 weeks after UNX. (d) Uniform capillary pattern, all capillaries are of fairly the same size. (e and f) Heterogenous capillary pattern; several dilated and abnormally shaped capillaries (arrows) are seen associated with a rearrangement of the corresponding mesangium (arrowheads). **(g–i)** Rats, 24 weeks after UNX. (g) Fairly uniform capillary pattern; only one distorted capillary profile is seen (arrow). (h and i) Heterogenous capillary pattern with several dilated capillary channels (arrows) and tuft appositions to Bowman's capsule (double arrows). The triangle points to an area with mesangial expansion (rarely encountered. VP, vascular pole. (a–f) ×~350; (g–i) ×~300.

animals, but the drop—despite a higher ERPF per kidney weight—was much steeper in UNX animals than in controls. In addition, 24 weeks after UNX a dramatic proteinuria was observed. Thus, filtration in the remnant glomeruli 24 weeks after UNX has become less effective than in controls, and there are substantial deteriorations in barrier function.

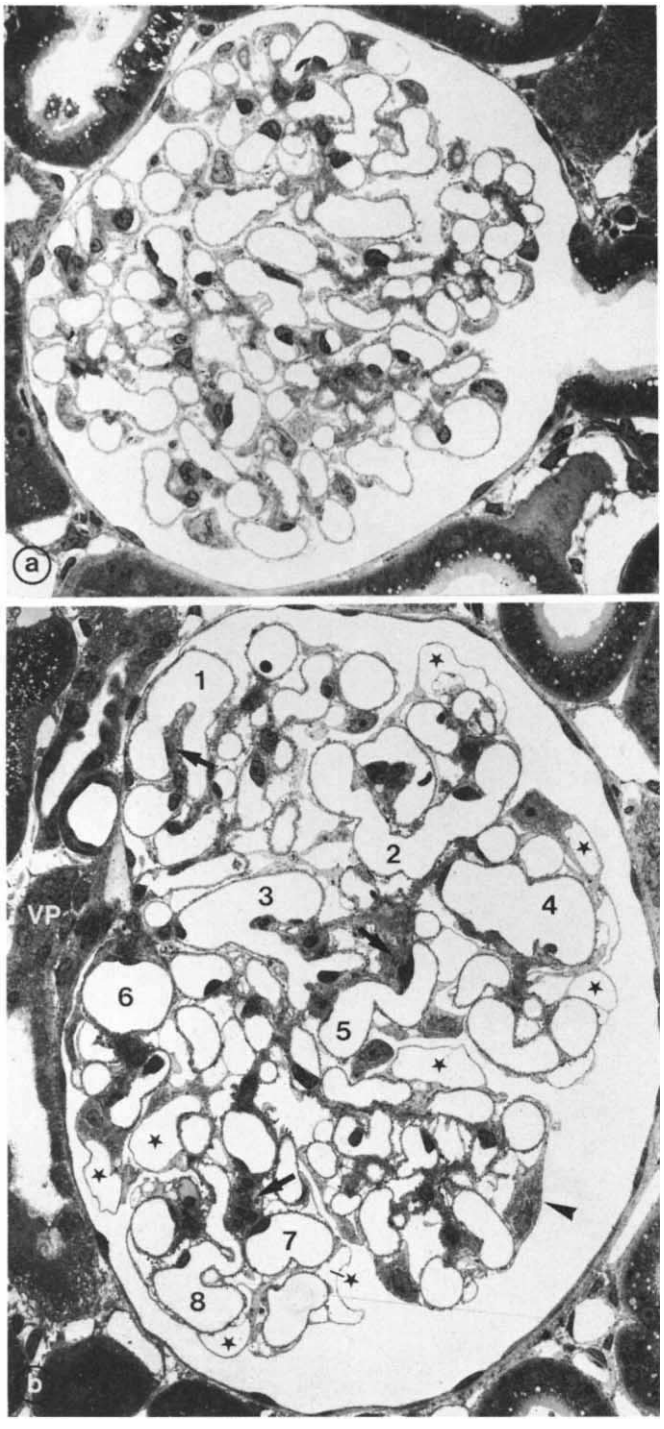

Fig. 4. *Transmission electron micrographs of whole glomerular profiles 24 weeks after surgery.* **(a)** Glomerulus of a sham-operated rat showing fairly uniform capillary profiles; no deteriorations in tuft structure are seen. **(b)** Glomerulus of an UNX rat exhibiting extensive distortions in tuft architecture. At least eight (1 to 8) abnormally shaped and dilated capillary channels are encountered; rearrangements of the corresponding mesangium are seen at three sites (arrows). Podocyte cellbodies are extensively hypertrophied (arrowhead); bleb formation (asterisks) is frequently encountered. VP, vascular pole. (a and b) ×~435.

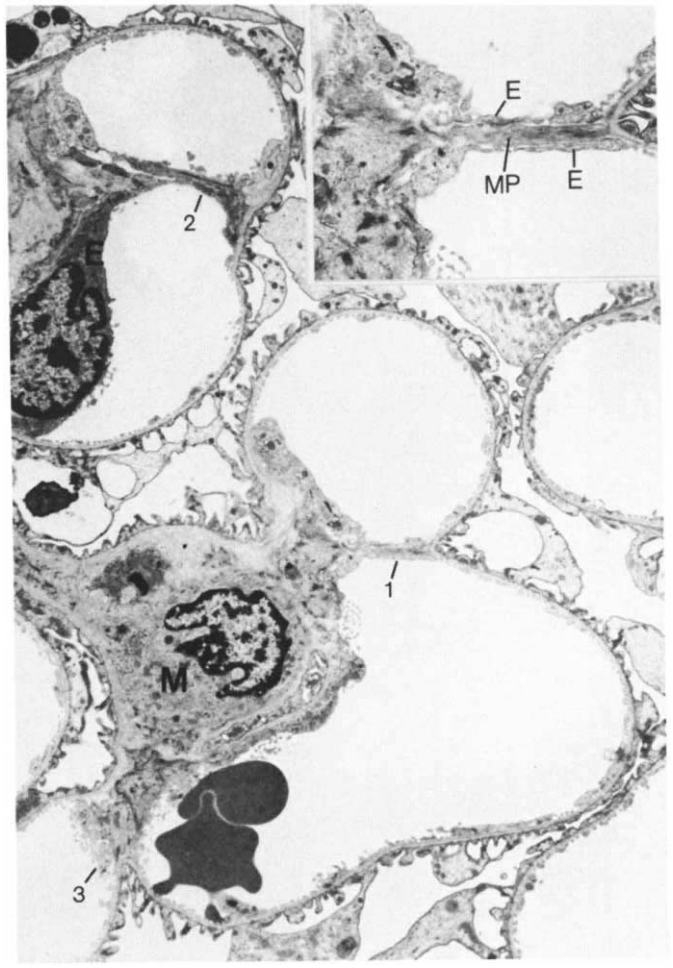

Fig. 5. *Transmission electron micrograph of abnormally shaped capillaries in a rat 24 weeks after UNX.* Immediate precursors of the coalescence of two capillaries into a single giant capillary are seen: the thin mesangial bridges (1, 2, 3) between two capillary profiles represent the outermost part of a mesangium which is in the process of retraction. The inlet shows an enlargement of (1): the thin mesangial bridge consisting of a mesangial cell process (MP) is complete covered on both sides by an endothelial layer (E). M, mesangial cell. ×~3800; inlet ×~8400.

Structural changes

The functional defects are accompanied by a considerable degree of structural damage in glomeruli of UNX animals. Although the frequency and severity of glomerulosclerosis seen in UNX animals was not extensive, the majority of glomeruli in UNX animals exhibited structural abnormalities. The present paper only deals with the changes in shape and size of capillaries.

Glomerular growth, normal and hypertrophic, leads to larger tufts with increased capillary length. As seen in Figure 2, which shows casts of glomeruli after normal (Fig. 2a) and hypertrophic growth (Fig. 2b), these glomeruli consist of capillary loops of a uniform type. All loops have about the same size; differences in capillary thickness between control and UNX rats are not obvious. On the other hand, as seen in SEM, LM and TEM (Figs. 2, 3 and 4), with time an increasing proportion of glomerular profiles

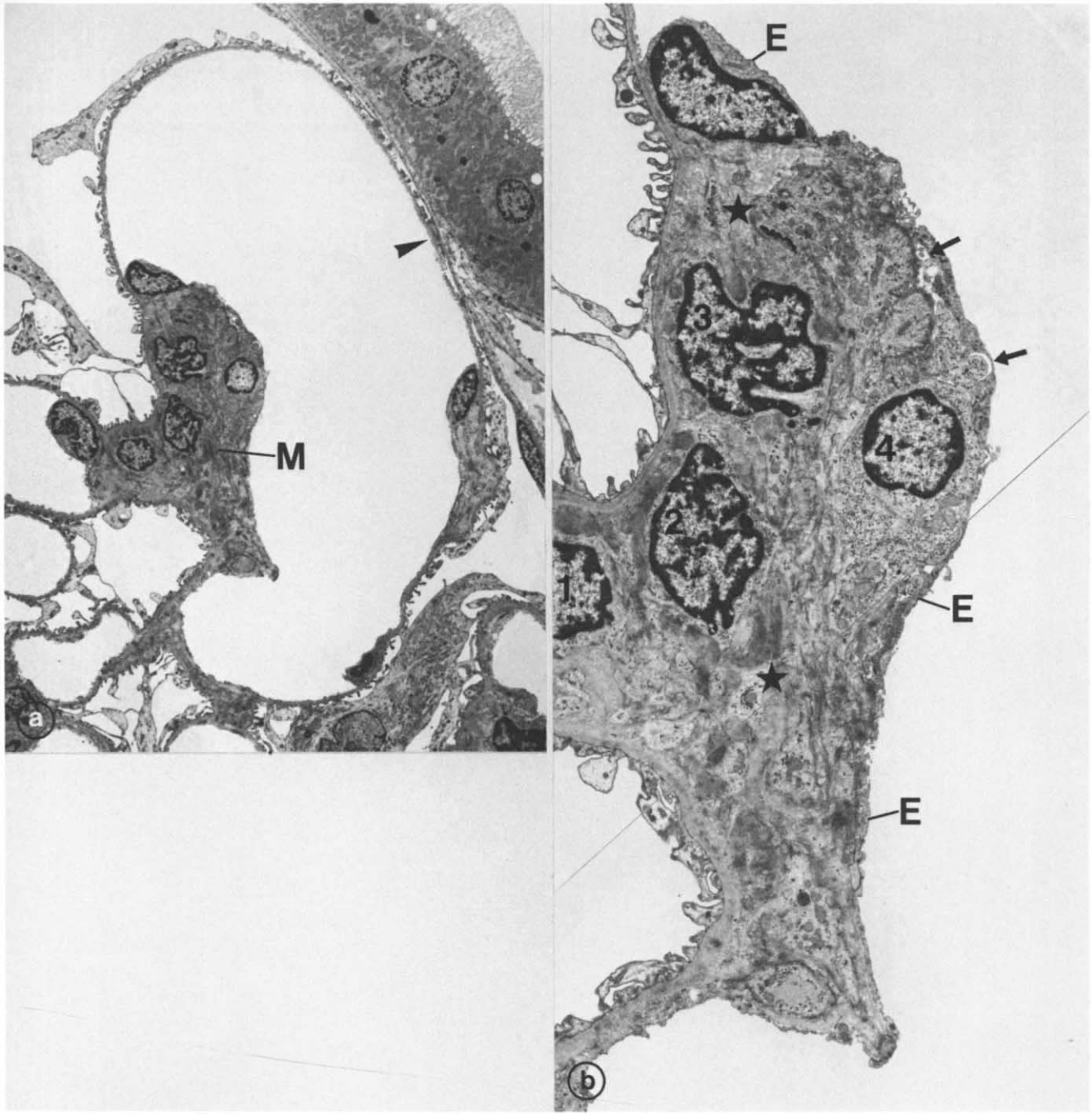

Fig. 6. *Transmission electron micrographs of a dilated capillary channel from the periphery of a tuft of a rat 24 weeks after UNX.* Note the apposition to Bowman's capsule (arrowhead). The channel is associated with a rearranged mesangium (M), which is shown enlarged in (b). Three mesangial cell bodies (1–3) and, probably, a macrophage (4) are seen. Towards the channel lumen the mesangium is completely covered by an endothelial layer (E), whose connections to the underlying elements appear to be loose (arrows). Abundant mesangial matrix is found (asterisks) consisting of homogenous as well as fibrillar material. (a) ×~1750; (b) ×~5500.

deviate in appearance from this uniform capillary pattern. Locally, individual capillary profiles appear quite unusual in shape and size. As shown in Figure 7, 24 weeks after surgery the incidence of glomeruli with such lesions had increased to 19% in controls and almost 50% in UNX animals. However, even in the glomerular profiles which showed such large vascular channels, the overwhelming majority of the capillaries were of a fairly uniform, small type. Thus, the appearance of these dilated and abnormally-shaped capillary channels represents a local event. We consider it to reflect not growth but rather dilation (see below).

The mesangium was not particularly prominent in the hypertrophied glomeruli. Even without a morphometric evaluation, it

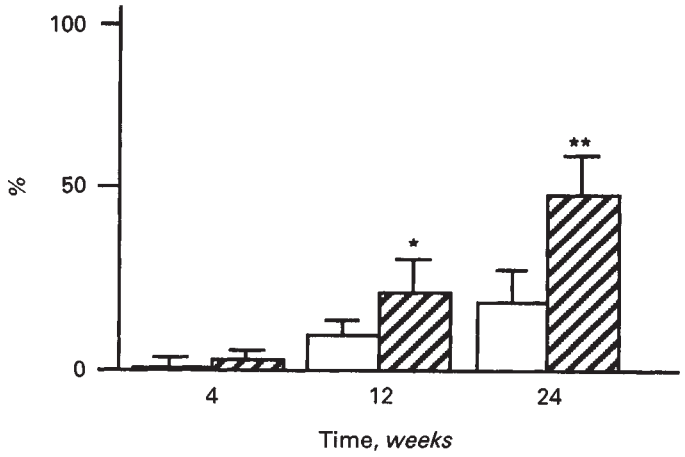

Fig. 7. *Frequency of heterogenous capillary pattern.* Compared to sham-operated rats (white bars), UNX rats (hatched bars) exhibit a much more pronounced increase of glomeruli with heterogenous capillary pattern. Number of animals: $N = 6$, except the 12 and 24 UNX weeks group with $N = 8$. $^{*}P < 0.05$, $^{**}P < 0.01$, sham-operated versus UNX animals within the same time group.

was clear that a disproportionate increase in mesangial area was not present. In agreement with a recent study by Schwartz and Bidani [28] hypertrophic glomerular growth in the present model was not associated with disproportionate mesangium growth. Mesangial expansion (that is, widening of a mesangial axis associated with hypercellularity and increased deposition of mesangial matrix) was only found in advanced stages of FGS, and then only in areas adherent to Bowman's capsule associated with established foci of sclerosis [1]. On the other hand, unusual assemblies of mesangial elements were often found associated with dilated capillaries. In our view, these local mesangial conglomerations do not represent mesangial expansion, but are the result of a mesangial rearrangement due to desertion by mesangial cells of their anchoring sites at the GBM. Together with capillary dilation, they represent the structural outcome of local mesangial failure.

Mesangial failure/capillary expansion

By mesangial failure we mean the local or generalized breakdown of the supporting function of the mesangium. It results either from insufficiency of mesangial contractility or from the disconnection of the mesangial contractile apparatus from its effector structure, the GBM. Mesangial failure may be followed by the expansion of either the mesangial or the capillary area. In the isolated perfused kidney, which may be used as a model to study acute mesangial failure [29], expansion is seen at both sites with a clear prevalence of capillary expansion. The giant capillary channels encountered in this model are very similar to those seen in the present study.

To understand the development of these abnormally shaped capillaries, a three-dimensional point of view is necessary. We have tried to sketch this process in Figure 8. Figure 8a shows a normal capillary loop. Stabilization of its shape is brought about by the centripetal pull of mesangial cells at their attachments to the GBM along the inner curve of the loop. Mesangial cell processes thus establish a series of "clamps" between opposing mesangial angles of the GBM parallel to the inner curve of the capillary [15]. Contractile insufficiency or disruption of these connections over a certain distance along a capillary loop will destabilize the capillary. Initially (Fig. 8b) a local ballooning of the capillary will be seen. As the mesangial damage proceeds, the capillary loop will also lose its curved shape and will straighten into a simpler and dilated capillary channel (Fig. 8c). The mesangium thereby retracts to a more axial position and piles up to form conspicuous mesangial conglomerations. A similar mechanism is thought to produce the dilated and distorted capillary channels in the isolated perfused kidney [29].

This process necessarily results in a rearrangement of mesangial material, also sketched in Figure 8b. At the end of this process parts of the mesangium are found in more axial positions, contacting the newly established capillary channels at quite unusual sites (Fig. 6). Within these rearranged mesangial areas the usual distribution of mesangial elements (cells, cell processes, matrix fibrils) is lost. Mesangial cells and cell processes frequently appear to be simply stacked together. This process of mesangial rearrangement is not associated with an increase in total mesangial space nor with cell proliferation, although, some *de novo* production of mesangial matrix within the redistributed areas may occur. It is important to recognize that these distortions in tuft structure take place without any disruptions of the capillary endothelium.

The way these changes in tuft structure are brought about may well bear similarities to the formation of microaneurysms as seen under experimental conditions characterized by a rapid rise in glomerular capillary pressure [16, 30] or after lysis of the mesangium as by the Habu snake venom [31, 32]. The expanded capillaries encountered in this model might in fact be regarded as precursors of a microaneurysm. However, the formation of microaneurysms is associated with extensive endothelial disruption [32], favoring the formation of capillary thrombosis. Organization of such a thrombus has been proposed to lead to segmental sclerosis [16]. Such a process was never seen in the present study.

Factors causing local mesangial failure in the present model

The formation of abnormally-shaped expanded capillary channels as seen in the present study is considered to be the result of a local failure of the supporting function of the mesangium. The failure may concern the contractile capacity of mesangial cells or the transmission of the contractile force to the GBM. The present study was not designed to discriminate between these two possibilities. A likely candidate as a causative factor would be insufficiency of the contractile capacity of the mesangial cells relative to the distending forces exerted to the GBM by the hydraulic pressure gradient across the GBM. The expansionary forces must be counteracted by wall tension, which—according to Laplace's law—not only increases with the pressure gradient but also with the radius of the vessel. Thus, the contractile challenge to the mesangium will increase with increasing capillary diameters as well as with increases in capillary pressure.

In fact, we found that dilated vascular channels appeared most often in the vicinity of the vascular pole. In reconstructions of the glomerular tuft [33, 34] it was noted that the primary intraglomerular branches of the afferent arteriole are distinctly larger than the majority of glomerular capillaries, but don't differ from them in wall structure. In glomerular casts of UNX

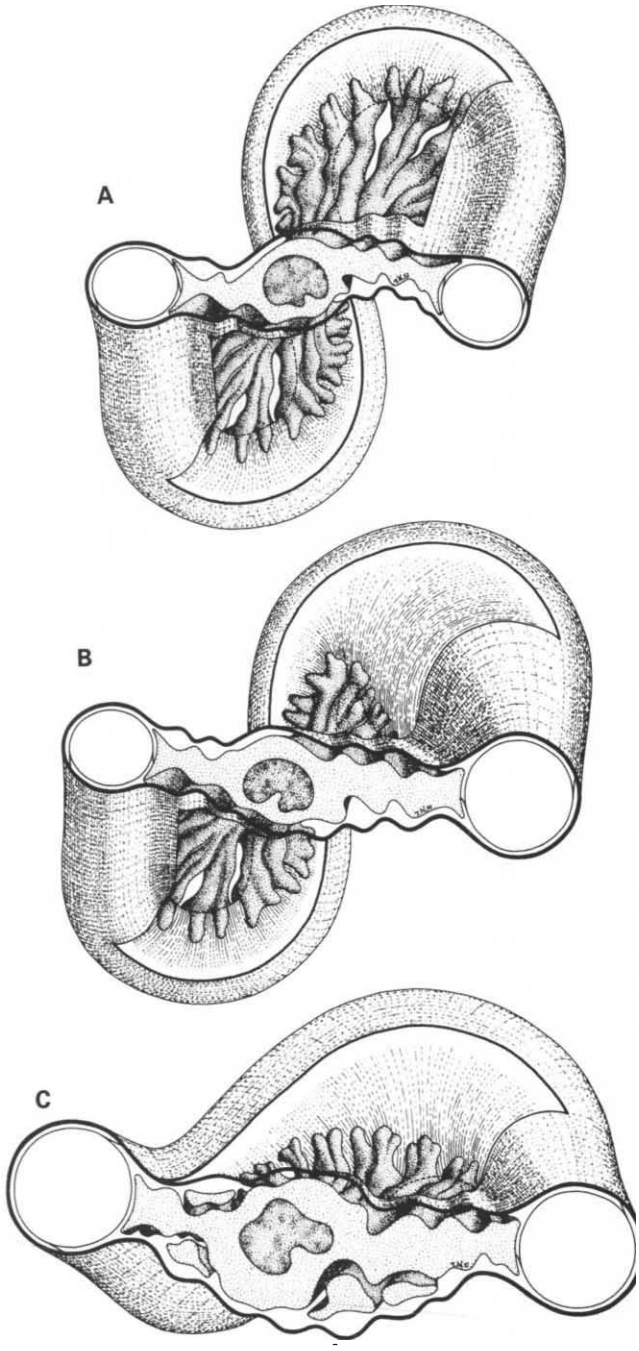

Fig. 8. *Schematic representation to show the process of capillary dilatation and mesangial retraction due to local mesangial failure.* (**a**) depicts a normal capillary loop together with an associated mesangial cell. The GBM cover is fenestrated to show the distribution of mesangial cell processes along the inner curve of the loop. These processes form a series of clamps which interconnect opposing parts of the GBM (indicated in the section plane by arrows) thereby guaranteeing the curved shape of the loop. (**b**) depicts a local dilatation in the upper part of this loop. Mesangial cell processes have become disconnected from their anchoring points at the GBM along a certain distance. As a consequence, the capillary expands and the mesangial cell retracts. (**c**) Progression of this process to adjacent portions of the capillary leads to a simplification of the capillary pattern and the formation of a dilated and abnormally-shaped capillary channel. The mesangium has moved into a centripetally located agglomeration.

animals primary branches were frequently found to be massively expanded (Fig. 2). These findings strongly suggest contractile insufficiency relative to increased wall tension as the crucial factor initiating the process of capillary expansion. Similar ideas have very recently been put forward by Daniels and Hostetter [35] to explain the previously noted prevalence of FGS to regions near the vascular pole [36, 37].

Relevance

The occurrence of abnormally shaped capillaries is not unique to the present model. Such capillaries are frequently seen in published photographs of glomeruli from the subtotal nephrectomy model [21, 28, 30, 38–41], but they have generally not been considered as pathologically important changes in tuft structure.

Apart from the specific model of mesangiolysis after Habu snake venom poisoning [32], microaneurysms are a rare event in experimental models leading to glomerulosclerosis. In human pathology they are rarely encountered. Therefore, the pathway to sclerosis via microaneurysms and thrombosis is generally considered to be only relevant to a small subset of cases of focal and segmental glomerulosclerosis [30]. From the present study we suggest that capillary ballooning (without endothelial disruption) may have pathogenetic relevance via a mechanism quite different from thrombosis. As shown in the accompanying paper [1], distortion of the capillary structure has important implications for the overlying podocytes also.

The formation of dilated capillary channels is not restricted to experimental animals. Such capillaries are also found in controls, albeit in much lower frequency. Counteracting capillary dilation probably is the principal function of the mesangium [42, 43]. It may be speculated that failure of this function accounts—at least in part—for the increasing glomerular obsolescence of the aging kidneys [44]. In glomeruli exposed to increased stress (hyperperfusion, hypertension) or in glomeruli with decreased stability (hypertrophy), the mechanism remains the same, the incidence only increases in frequency.

Acknowledgments

This study was supported by Deutsche Forschungsgemeinschaft, Forschergruppe "Niere" Heidelberg, grant Kr 546/5-3. We thank Ms. Hiltraud Hosser, Ms. Bruni Hähnel and Ms. Ingrid Hartmann for skillful technical assistance. The excellent photographical work by Ms. Ingrid Ertel and elegant graphic work by Mr. Rolf Nonnenmacher are gratefully acknowledged. Logistic and secretarial help was provided by Ms. Helene Dehoust. We also thank Dr. Kevin Lemley for his valuable criticism and help in preparing this manuscript. Dr. A.P. Provoost and Mr. A. van Aken (Department of Pediatric Surgery, Erasmus University, Rotterdam) as well as Dr. B. Bubeck (Radiologische Universitäts-Klinik Heidelberg) instructed us how to do the GFR and ERPF measurements; their help is gratefully acknowledged. Part of this study has been presented at the annual meeting of the "Gesellschaft für Nephrologie," 1990 (Badgastein), and at the congress of the "European Society of Pediatric Nephrology," 1990 (Rome).

Reprint requests to Prof. Dr. Wilhelm Kriz, Institut für Anatomie und Zellbiologie I, Im Neuenheimer Feld 307, 6900 Heidelberg, Germany.

References

1. Nagata M, Kriz W: Glomerular damage after uninephrectomy in young rats. II. Mechanical stress on podocytes as a pathway to sclerosis. *Kidney Int* 42:148–160, 1992
2. Fogo A, Ichikawa I: Evidence of central role of glomerular

growth promoters in the development of sclerosis. *Semin Nephrol* 9:329–342, 1990
3. YOSHIDA Y, KAWAMURA T, IKOMA M, FOGO A, ICHIKAWA I: Effects of antihypertensive drugs on glomerular morphology. *Kidney Int* 36:626–635, 1989
4. KAUFMANN JM, HARDY R, HAYSLETT JP: Age dependent characteristics of compensatory renal growth. *Kidney Int* 8:21–26, 1975
5. O'DONNELL MP, KASISKE BL, RAJE L, KEANE WF: Age is a determinant of the glomerular morphologic and functional processes to chronic nephron loss. *J Lab Clin Med* 106:308–313, 1985
6. CELSI G, BOHMAN SO, APERIA A: Development of focal glomerulosclerosis after unilateral nephrectomy to infant rats. *Pediatr Nephrol* 1:290–296, 1987
7. CELSI G, LARSSON L, SERI I, SAVIN V, APERIA I: Glomerular adaptation in uninephrectomized young rats. *Pediatr Nephrol* 3:280–285, 1989
8. OKUDA S, MOTOMURA K, SANAI T, TSURUDA H, OH Y, ONOYAMA K, FUJISHIMA M: Influence of age on determination of the remnant kidney in uninephrectomized rats. *Clin Sci* 72:571–576, 1987
9. RICCIARELLI G: *Morphologische Untersuchungen zur postnatalen Entwicklung der Rattenniere*. (Dissertation) Westfälische, Wilhelms-Universität Münster, 1969, pp. 31
10. PROVOOST AP, KEIJZER MH, WOLFF ED, MOLENAAR JC: Development of renal function in the rat. The measurement of GFR and ERPF and correlation to body and kidney weight. *Renal Physiol* 6:1–9, 1983
11. BAINES AD, ROUFFIGNAC CDE: Functional heterogeneity of nephrons. II. Filtration rates, intraluminal flow velocities an fractional water reasorption. *Pflügers Arch* 308:260–276, 1969
12. LARSSON L, MAUNSBACH AB: The ultrastructural development of the glomerular filtration barrier in the rat kidney: a morphometric analysis. *J Ultrastruct Res* 72:392–406, 1980
13. LOTT JA, STEPHAN VA, PRITCHARD KA: Evaluation of the Coomassie Brilliant Blue G-250 method for urinary protein. *Clin Chem* 29:1946–1950, 1984
14. KAISSLING B, KRIZ W: Variability of intercellular spaces between macula densa cells: A transmission electron microscopic study in rabbits and rats. *Kidney Int* 12:S9–S17, 1982
15. SAKAI T, KRIZ W: The structural relationship between mesangial cells and basement membrane of the renal glomerulus. *Anat Embryol* 176:373–386, 1987
16. DWORKIN LD, HOSTETTER TH, RENNKE HG, BRENNER BM: Hemodynamic basis for glomerular injury in rats with desoxycorticosterone-salt hypertension. *J Clin Invest* 73:1448–1461, 1984
17. FRIES JW, SANDSTROM DJ, MEYER TW, RENNKE HG: Glomerular hypertrophy and epithelial cell injury modulate progressive glomerulosclerosis in the rat. *Lab Invest* 60:205–218, 1989
18. MILLER PL, MEYER TW: Methods in laboratory investigation. Effects of tissue preparation on glomerular volume and capillary structure in the rat. *Lab Invest* 63:862–866, 1990
19. ELGER M, SAKAI T, KRIZ W: Role of mesangial cell contraction in adaptation of the glomerular tuft to changes in extracellular volume. *Pflügers Arch* 415:598–605, 1990
20. WEIBEL ER: *Stereological Methods. Practical Methods for Biological Morphometry*. London, Academic Press, 1979
21. HOSTETTER TH, OLSON JL, RENNKE HG, VENKATACHALAM MA, BRENNER BM: Hyperfiltration in remnant nephrons: A potentially adverse response to renal ablation. *Am J Physiol* 241:F85–F93, 1981
22. KIPROV DD, COLVIN RB, MCCLUSKEY RT: Focal and segmental glomerulosclerosis and proteinuria associated with unilateral renal agenesis. *Lab Invest* 46:275–282, 1982
23. FOGO A, YOSHIDA Y, GLICK AD, ICHIKAWA I: Serial micropuncture analysis in two rat models of glomerulosclerosis. *J Clin Invest* 82:322–330, 1988
24. JELINEK J, HACKENTHAL E, HACKENTHAL R: Role of the renin-angiotensin-system in adaptation to high salt intake in immature rats. *J Develop Physiol* 14:89–94, 1990
25. MACKEY K, STRIKER LJ, STAUFFER JW, AGODOA LY, STRIKER G: Relationship of glomerular hypertrophy and sclerosis: Studies in SV 40 transgenic mice. *Kidney Int* 37:741–748, 1989
26. DOI T, STRIKER LJ, GIBSON CC, AGODOA LY, BRINSTER RL, STRIKER GE: Glomerular lesions in mice transgenic for growth hormone and insuline-like growth factor-I. I. Relationship between increased glomerular size and mesangial sclerosis. *Am J Pathol* 137:541–552, 1990
27. PROVOOST AP, KEIJZER MH, MOLENAAR JC: Effect of protein on lifelong changes in renal function of rats unilaterally nephrectomized at young age. *J Lab Clin Med* 114:19–26, 1989
28. SCHWARTZ MM, BIDANI AK: Mesangial structure and function in the remnant kidney. *Kidney Int* 40:226–237, 1991
29. SAKAI T, LEMLEY KV, HACKENTHAL E, NAGATA M, NOBILING R, KRIZ W: Changes in glomerular structure following acute mesangial failure in the isolated perfused kidney. *Kidney Int* 41:533–541, 1992
30. RENNKE HG, ANDERSON S, BRENNER BM: Structural and functional correlations in the progression of kidney disease, in *Renal Pathology*, edited by TISHER CC, BRENNER BM, Philadelphia, Lippincott, 1989, p. 43
31. MORITA T, KIHARA I, OITE T, YAMAMOTO T, SUZUKI Y: Mesangiolysis. Sequential ultrastructural study of Habu venom-induced glomerular lesions. *Lab Invest* 38:94–102, 1978
32. MORITA T, CHURG J: Mesangiolysis. *Kidney Int* 24:1–9, 1983
33. LAMBERT PP, AIKENS B, BOHLE A, HANUS F, PEGOFF S, VAN DAMME M: A network model of glomerular function. *Microvasc Res* 23:99–128, 1982
34. WINKLER D, ELGER M, SAKAI T, KRIZ W: Branching and confluence pattern of glomerular arterioles in rat. *Kidney Int* 39 (Suppl 32):S2–S8, 1991
35. DANIELS BS, HOSTETTER TH: Adverse effects of growth in the glomerular microcirculation. *Am J Physiol* 258:F1409–F1416, 1990
36. ELEMA JD, ARENDS A: Focal and segmental glomerular hyalinosis and sclerosis in the rat. *Lab Invest* 33:554–561, 1975
37. GROND J, SCHILTHUIS MS, KONDSTAAD J, ELEMA JD: Mesangial function and glomerular sclerosis in rats after UNX. *Kidney Int* 22:338–343, 1982
38. OLSON JL, HOSTETTER TH, RENNKE HG, BRENNER BM, VENKATACHALAM MA: Altered glomerular permselectivity and progressive sclerosis following extreme ablation of renal mass. *Kidney Int* 22:112–126, 1982
39. HOSTETTER TH, MEYER TW, RENNKE HG, BRENNER BM: Chronic effects of dietary protein in the rat with intact and reduced renal mass. *Kidney Int* 30:509–517, 1986
40. GRISHMAN E, CHURG J: Focal glomerular sclerosis in nephrotic patients: An electron microscopic study of glomerular podocytes. *Kidney Int* 7:111–122, 1975
41. DOI T, HATTORI M, AGODOA LYC, SATO T, YOSHIDA H, STRIKER LJ, STRIKER GE: Glomerular lesions in nonobese diabetic mouse: Before and after the onset of hyperglycemia. *Lab Invest* 63:204–212, 1990
42. KRIZ W, ELGER M, LEMLEY KV, SAKAI T: Structure of the glomerular mesangium: A biomechanical interpretation. *Kidney Int* 38 (Suppl 30):S2–S9, 1990
43. KRIZ W, ELGER M, LEMLEY KV, SAKAI T: Mesangial cell-glomerular basement membrane connections counteract glomerular capillary and mesangium expansion. *Am J Nephrol* 10:4–13, 1990
44. ANDERSON S, BRENNER BM: Effects of aging on the renal glomerulus. *Am J Med* 80:435–442, 1986